

Optimization of Process Parameters for AISI 304 Using Micro-EDM Drilling Process Through Response Surface Method

Jinesh B. Shah^{1*}, Kailashkumar P. Vala²

Abstract

The increasing demand for micro-parts in high-tech products, such as micro-electromechanical systems (MEMS) applications and micro-electronic devices, has driven significant advancements in micromachining technologies. Among the various micromachining processes, the fabrication of accurate microholes and pins is critical for the performance and reliability of miniature components. Micro-hole drilling plays a vital role by enabling the production of deep holes with excellent straightness, roundness, and surface quality. It is widely used in precision industries, including the manufacturing of watch components, camera parts, and automotive fuel injection nozzles. Electrical discharge machining (EDM), a non-contact machining process suitable for electrically conductive materials, is highly effective for producing high aspect ratio holes and is extensively utilized in the tool and die manufacturing sector. This study focuses on investigating the micro-EDM drilling process parameters for machining AISI 304 stainless steel using a 1 mm diameter brass electrode. The key input parameters analyzed are peak current (I_p), pulse-on-time (T_{on}), and pulse-off-time (T_{off}), while the primary output responses are tool wear rate (TWR) and material removal rate (MRR). A central composite design (CCD) combined with response surface methodology (RSM) has been employed to develop predictive models for performance characteristics. A three-level full factorial experimental design was implemented to systematically study the influence of drilling parameters. Multi-response optimization was carried out using the desirability function approach to identify the optimal combination of machining parameters that simultaneously minimize tool wear and maximize material removal rate. Finally, experimental validation of the optimized conditions will be conducted to confirm the effectiveness and reliability of the developed models. The findings of this study are expected to contribute to improved efficiency and precision in micro-EDM drilling processes for industrial applications.

Keywords: EDM drill, AISI304, material removal rate, tool wear rate, RSM, optimization.

*Author for Correspondence

Jinesh B. Shah

E-mail: jinesh.shah@atmiyauni.ac.in

¹Assistant Professor, Department of Mechanical Engineering, Atmiya University, Rajkot, Gujarat, India

²Research Scholar, Department of Mechanical Engineering, Atmiya University, Rajkot, Gujarat, India

Received Date: March 26, 2025

Accepted Date: May 14, 2025

Published Date: May 24, 2025

Citation: Jinesh B. Shah, Kailashkumar P. Vala. Optimization of Process Parameters for AISI 304 Using Micro-EDM Drilling Process Through Response Surface Method. International Journal of Manufacturing and Production Engineering. 2025; 3(1): 37–47p.

INTRODUCTION

Since its development in the 1940s, electrical discharge machining (EDM), one of the most popular nonconventional machining techniques, has been extensively utilized in the manufacturing of hard and electrically conductive materials that are difficult to cut. During the EDM process, material removal from the workpiece occurs because of the intense heat generated by numerous high-frequency electrical sparks within a small gap between the tool electrode and the workpiece. Unlike traditional computer numerical control (CNC) machining, EDM is a thermal-based process in which the tool

and workpiece do not make physical contact. Consequently, common issues in conventional machining, such as chatter, vibration, and mechanical stresses, are completely eliminated. EDM can machine any electrically conductive material, irrespective of its mechanical properties such as strength or hardness. These advantages make EDM particularly valuable for manufacturing, aerospace, and biomedical industries, where there is a high demand for components made from difficult-to-machine materials. Applications include the production of cutting tools, turbine blades, implants, and artificial joints, which are often made from materials such as polycrystalline diamonds, nickel-based alloys, and titanium alloys. These materials are favored because of their exceptional ability to withstand high temperatures and mechanical stresses during operation under challenging conditions [1].

Drilling is a crucial machining procedure in the manufacturing sector. Different types of holes are drilled in conventional machining operations using spinning drill bits of various shapes. It is challenging to drill good-quality holes in hard-to-cut materials, especially deep holes, because of the high strength of the material, low stiffness of the drill bits, poor cooling effects of the process, and challenges associated with chip expelling. Additionally, the possibility of drill bit breaking or twisting makes drilling holes with a large aspect ratio and microholes much more challenging. Therefore, to create hole features, particularly those with small diameters and big aspect ratio holes on difficult-to-cut materials, electrical discharge drilling, or EDM, technology is utilized employing cylindrical electrodes by altering the electrode's form, it can also be used to create holes in intricate geometries with non-circular cross-sections. In this instance, the technique is known as electrical discharge hole creation, because the electrode moves differently than it does during drilling. For example, specialized facilities built around EDM machines can be used to produce curved and square holes. Despite EDD's significant improvements in EDD over traditional methods, there are several underlying issues. For instance, when drilling holes in a workpiece made of conventional materials, its machining efficiency is lower than that of the CNC method. Additionally, the holes created by EDD may have geometric errors, such as overcut (OC) and taper, high residual stress, and thermal defects, such as the recast layer. These issues lead to lower-quality holes and higher production costs. To increase the quality of holes produced by EDD and the efficiency of machining, a significant amount of research has been conducted in this field. However, an in-depth understanding of these challenges is lacking, and the underlying processes of these problems have not been well examined [2].

EDM is one of the most important and widely used nonconventional machining techniques, particularly owing to its ability to machine complex shapes and hard-to-cut materials with high precision. Other names for electrical discharge machining include wire burning or wire erosion, die sinking, spark machining, and spark erosion. Hard materials and electrically conductive alloys that can withstand high temperatures are typically machined using this method. The EDM technique operates by utilizing thermoelectric energy to generate rapid, repetitive sparks between a non-contacting electrode and the workpiece, resulting in the erosion of electrically conductive materials [3].

It is a non-traditional electrothermal machining technology in which electrical energy is employed to create an electrical spark. Material removal in EDM occurs through a sequence of rapid current discharges between the two electrodes separated by a dielectric fluid. Difficult geometries can be machined in small quantities or even on a job-shop basis [4].

Many studies have addressed EDM procedures with various goals. The development of extremely durable electrically conductive materials such as carbides, stainless steels, Hastelloy, nitralloys, and waspalloys has increased the need for unconventional manufacturing techniques [12]. These highly durable materials are extremely challenging to process using traditional techniques. They have many uses, including the production of dies and automotive and aerospace components [5].

Regardless of the hardness and toughness of the materials, EDM procedures heavily utilize thermal energy to machine electrically conductive materials. EDM offers considerable potential in nonconventional

machining techniques owing to its versatility and utilization across modern sectors [5]. Through the controlled application of high-frequency electrical discharges, EDM can create holes, external shapes, profiles, and cavities in electrically conductive workpieces by melting or vaporizing materials at specific locations. During this process, the tool electrode (cathode) and workpiece (anode) are subjected to controlled direct-current pulses, resulting in precisely localized electrical discharges that facilitate material removal [6].

EXPERIMENTAL WORK

Material and Process

Hole drilling using EDM is a highly specialized technique developed to drill deep, small-diameter holes into electrically conductive materials. This process is particularly effective for producing precision holes with high aspect ratios, even for hard-to-machine or heat-resistant materials [7].

For the experiment, an AISI 304 (65×30×30 mm) was used, which was drilled using a brass electrode with a diameter of 1 mm. The machine used for this experiment was a Chmer CM H30A ø0.2 - ø3.0 X 400MM. The dielectric fluid is water.

DESIGN OF EXPERIMENT

Experimental Design (ED) and Design of Experiments (DOE) are crucial stages in the Statistical Process Control (SPC) process. This involves the use of different experimental designs to obtain optimal results. These designs can be represented quantitatively to optimize the parameters and enhance the overall performance. Tables 1 and 2 show the chemical and physical composition of AISI 304.

Central composite design (CCD) is a specific type of response surface design employed in studies aimed at determining the optimal values for multiple independent variables or components. The CCD incorporates three types of experimental variables: factor levels, axial points, and center points. This design was utilized to efficiently explore and analyze the relationships between variables and identify the best settings for achieving the desired outcomes. Table 3 shows the total number of experiments performed using the Design Expert software.

Table 1. Chemical composition of AISI 304.

S.N.	Element	Percentage
1	C	0.08 (max)
2	Mn	2.00 (max)
3	Si	1.00 (max)
4	Cr	18.0–20.0
5	N	0.10 (max)
6	Ni	8.0–10.5
7	P	0.045 (max)
8	S	0.030 (max)

Table 2. Physical properties of AISI 304 [8].

Properties	Req. value
Density [g/cm ³]	8.03
Melting temperature (Tw) [°C]	1455
Electrical resistivity (ρw) [Ωcm]	73
Thermal conductivity (kw) [W/mK]	16.3
Specific heat [J/(g°C)]	0.5

Table 3. Mechanical properties of AISI 304 [9]

Properties	Req. value
Tensile strength (MPa) min	515
Yield strength 0.2% Proof (MPa) min	205
Hardness Rockwell (HR) max	92
Hardness Brinell (HB) max	201
Elongation in 50 mm min %	40

OPTIMIZATION AND VALIDATION

The optimization process typically involves defining the problem, identifying the objective function, specifying the constraints, and selecting an appropriate optimization method. Common optimization methods include gradient-based algorithms, evolutionary algorithms, linear programming, and heuristic approaches. Optimization refers to the process of determining the best possible solution or a set of parameter values for a given objective function while adhering to defined constraints or specified requirements. The objective may vary depending on the context, such as maximizing profit, minimizing cost, or optimizing system performance. Optimization techniques utilize mathematical algorithms, modeling, simulation, and statistical methods to search for an optimal solution within a defined parameter space.

On the other hand, validation is the process of confirming the accuracy, reliability, and effectiveness of a model, system, or solution. It evaluates whether the optimized outcome meets the intended objectives and performs as expected under real-world conditions. This is typically achieved by comparing the results of the optimized solution with empirical data, experimental observations, or established benchmarks.

RESPONSE SURFACE METHOD AND CONFIRMATION

Once a response surface model is established, it can serve multiple purposes. These include predicting the response for untested input variable combinations, determining the optimal settings of the input variables to achieve the desired response, and performing sensitivity analyses to assess the relative significance of different variables. By constructing a response surface model and utilizing statistical analysis tools, RSM enables efficient experimentation, prediction, optimization, and improvement of processes or systems.

Confirmation is a critical step in scientific methods and research processes. The process of confirmation involves conducting additional experiments or studies to replicate the original findings. These replication attempts can be performed by the original researchers or by independent researchers to ensure objectivity and eliminate bias. The confirmation process may also involve different methodologies, sample sizes, or experimental conditions to strengthen the robustness of the findings. The primary objective of confirmation was to assess the consistency and reliability of the original results. If replication studies yield similar outcomes, they provide confidence in the validity and generalizability of initial findings. Confirmation involves replication and verification of the experimental findings or results to ensure their reliability, validity, and reproducibility.

RESULT AND DISCUSSION

In this study, three input parameters and two output parameters are involved in this current work. The results of the output responses are discussed below.

Experimental Data Analysis

The design of the experiment was created with the help of a central composite design in the Design Expert software, and given a combination of data. Table 4 presents the design of the experiment with the responses, and Table 5 presents the design of the experiment combination.

Table 4. Drilling parameters and their range.

Parameters	Low	Medium	High
Pulse-on-time (Ton)	3	6	9
Pulse-off-time (Toff)	2	3	4
Peak current (Ip)	5	7	9

Table 5. Design of experiment combination.

Exp. no.	Peak current (Ampere)	Pulse-on time (μ s)	Pulse-off time (μ s)
1	5	6	3
2	5	9	2
3	7	3	3
4	7	6	3
5	7	6	3
6	7	6	3
7	5	3	4
8	9	9	2
9	9	6	3
10	5	9	4
11	7	6	3
12	7	6	4
13	9	3	4
14	9	3	2
15	7	6	3
16	7	9	3
17	7	6	3
18	7	6	2
19	9	9	4
20	5	3	2

Response Discussion

A response discussion is essential for the analysis and behavior of the output responses. In this study, two output responses are considered: MRR and TWR. Some 3D surface plots represent the output-response analysis.

Figure 1 shows the interaction graph of the peak current (Ip) and pulse-on-time (Ton) for the MRR. The material removal rate increased linearly as the pulse current increased. This is because the energy intensity of a spark increases quickly, producing a large amount of thermal energy that causes the materials in the workpiece to melt and vaporize. Moreover, when the pulse-on-time increases from 6 to 9 μ s, the MRR increases rapidly. This is because a higher pulse on-time leads to a higher amount of material removal from the workpiece because thermal energy takes a longer time to penetrate the workpiece, causing melting and increasing the material removal. Table 6 presents the ED with the output responses. These results are similar to those obtained in the micro-EDM process by other researchers [10, 11].

The interaction between the peak current (Ip) and the pulse-off-time (Toff) on the MRR is shown in Figure 2. As the current increased, the MRR increased significantly at low Toff levels and progressively decreased as Toff increased. This phenomenon could be attributed to the increased heat loss with increasing Toff, longer machining times, and a decrease in spark frequency. All of these factors combined

Factor coding: Actual

Material removal rate ($\text{mm}^3/\text{min.}$)

Design points:

● Above surface

○ Below surface

3.899  15.3

X1 = A

X2 = B

Actual factor

C = 3

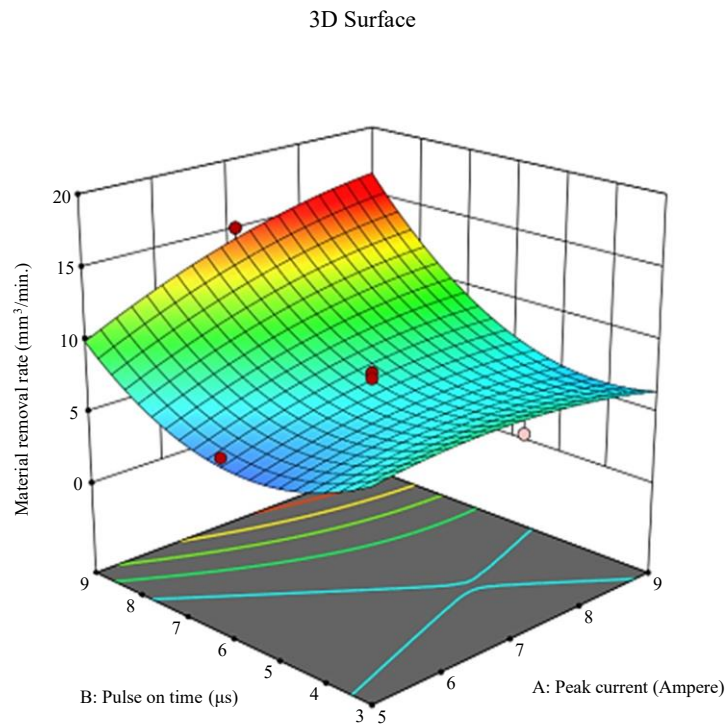


Figure 1. 3D surface plot of peak current and pulse-on-time for MRR.

Table 6. Design of experiment with output responses.

Run	Ip	Ton	Toff	MRR ($\text{mm}^3/\text{min.}$)	TWR ($\text{mm}^3/\text{min.}$)
1	5	6	3	5.548	2.305
2	5	9	2	11.387	5.827
3	7	3	3	7.146	2.942
4	7	6	3	7.081	2.63
5	7	6	3	7.066	2.798
6	7	6	3	7.025	2.875
7	5	3	4	5.259	2.107
8	9	9	2	15.3	11.89
9	9	6	3	6.862	2.855
10	5	9	4	4.817	1.72
11	7	6	3	7.85	2.82
12	7	6	4	6.148	2.602
13	9	3	4	6.878	2.908
14	9	3	2	3.899	1.324
15	7	6	3	7.41	2.977
16	7	9	3	15.1	10.69
17	7	6	3	7.82	2.74
18	7	6	2	5.266	1.595
19	9	9	4	14.82	10.75
20	5	3	2	6.907	2.315

led to a reduction in the material removal rate. pulse-off-time increases until 3(μs) MRR increases after the pulse-off-time MRR decreases slowly. These results are similar to those obtained in the micro-EDM process by other researchers [12].

Factor coding: Actual

Material removal rate ($\text{mm}^3/\text{min.}$)

Design points:

● Above surface

○ Below surface

3.899  15.3

X1 = A

X2 = C

Actual factor

B = 6

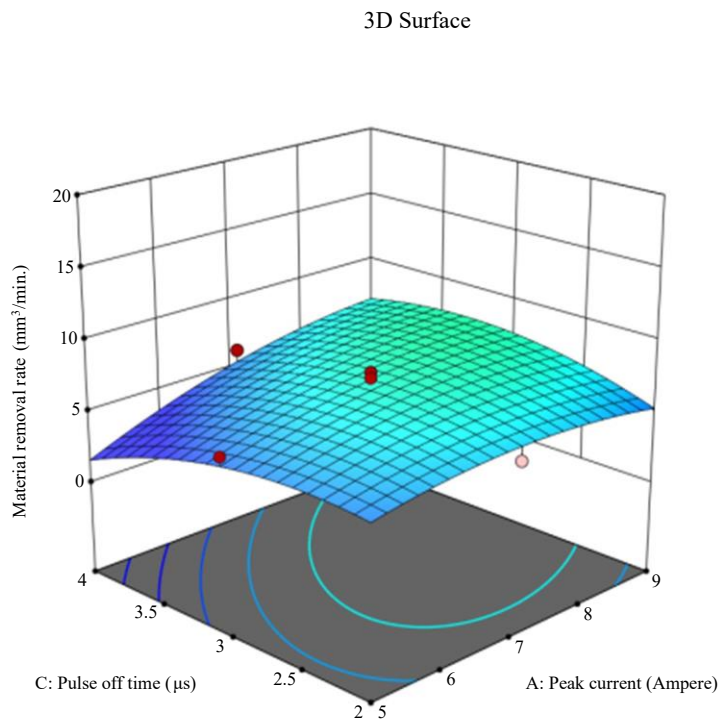


Figure 2. 3D surface plot of peak current and pulse-off-time for MRR.

Factor coding: Actual

Tool wear rate ($\text{mm}^3/\text{min.}$)

Design points:

● Above surface

○ Below surface

1.324  11.89

X1 = A

X2 = C

Actual factor

B = 6

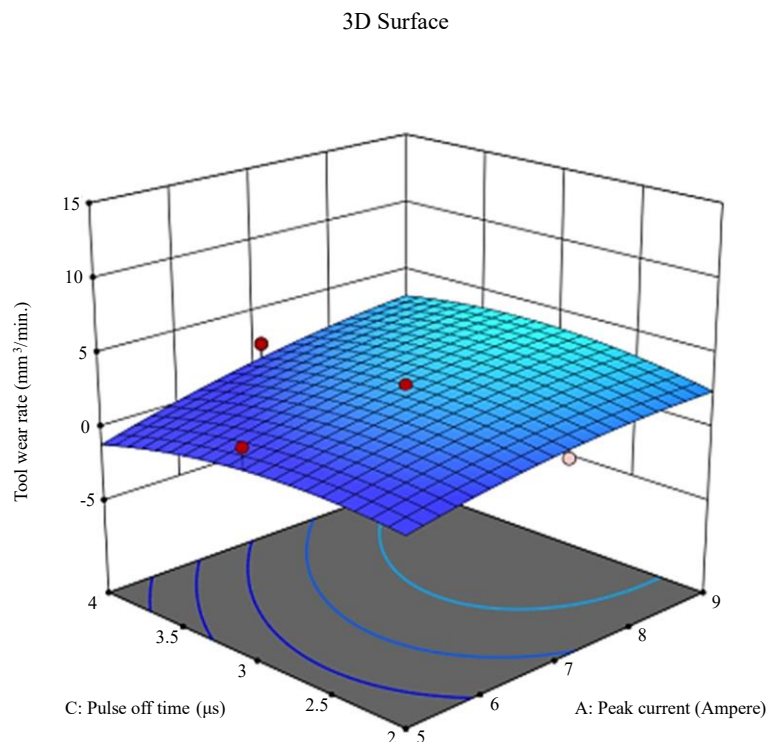


Figure 3. 3D surface plot of peak current and pulse-off-time for TWR.

The interaction between the peak current (I_p) and pulse-off-time (T_{off}) on the TWR is shown in Figure 3. It is noted that for all peak current values, the TWR increases as the current increases. In addition, it was observed that TWR progressively decreased as T_{off} increased. This is because there

Factor coding: Actual

 Tool wear rate ($\text{mm}^3/\text{min.}$)

Design points:

● Above surface

○ Below surface

 1.324  11.89

X1 = A

X2 = B

Actual factor

C = 3

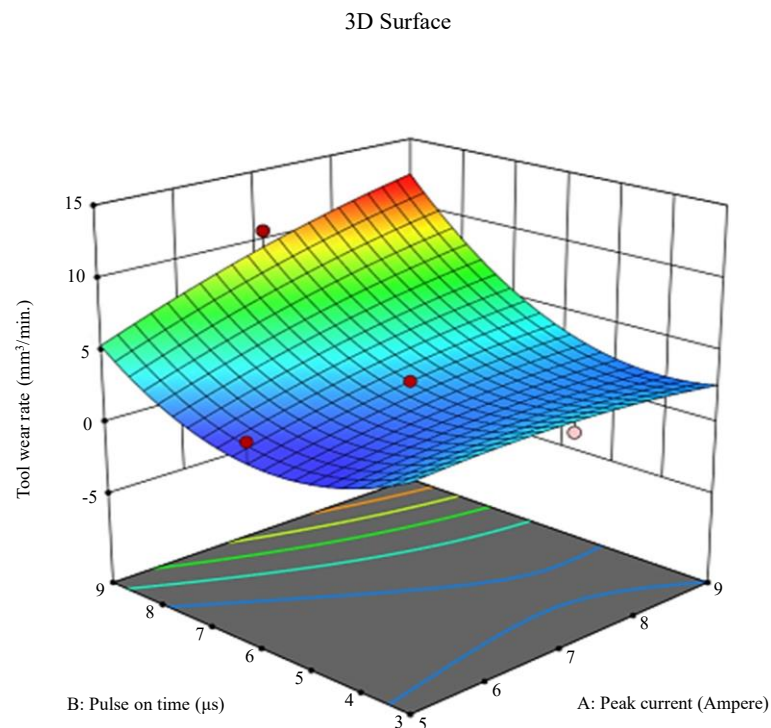


Figure 4. 3D surface plot of peak current and pulse-on-time for TWR.

was less sparking energy and sufficient time for the electrode to cool down. However, a slight increase in TWR was also observed at higher levels of peak current (I_p) (i.e., greater than $7 \mu\text{s}$). This may occur because, at higher T_{off} values, there is more variation in both the thermal and spark energy. Consequently, the establishment of the plasma channel requires more energy, which increases electrode wear. These results are similar to those obtained in the micro-EDM process by other researchers [13].

A remarkable correlation between the peak current and pulse-on-time was observed in the material, as illustrated in the 3D surface plot (Figure 4). The electrode wear rate increased proportionally with the increase in current after $7(\mu\text{s})$ of T_{on} . This phenomenon is explained by the fact that when the current increases, more charged particles, such as ions and electrons, are released at the contact between the tool electrode and the workpiece. High current levels produce significant heat generation at the electrode surface owing to the movement of high-energy charges in the plasma channel, which increases electrode wear. It is also observed from Figure 4 that there is a gradual increase in the tool wear rate with an increase in the pulse on-time. This could be the result of a longer sparking period, which softens the electrode material and produces high heat energy. These results are very similar to those obtained in the micro-EDM process by other researchers [14, 15].

Model Fitting

In regression analysis, model fitting refers to the process of estimating the parameters of the regression model based on available data. The objective is to identify the most suitable model that effectively represents the relationship between the dependent and independent variables, ensuring a good fit for the data. The regression equation for both the output responses is as follows:

1. Regression equation of MRR

$$\begin{aligned} \text{Material Removal Rate} = & +7.90633 + 0.389601 * \text{Peak current} - 5.31810 * \text{Pulse-on-time} + 6.11677 \\ & + \text{Pulse-off-time} + 0.318854 * \text{Peak current} * \text{Pulse-on-time} + 0.669812 * \text{Peak current} * \text{Pulse-} \\ & \text{off-time} - 0.258580 * \text{Peak current}^2 + 0.431520 * \text{Pulse-on-time}^2 - 1.53232 * \text{Pulse-off-time}^2 \end{aligned}$$

The equation in terms of actual factors can be used to predict the response for the given levels of each factor. The levels should be specified in the original units for each factor.

2. Regression equation of TWR

$$\text{Tool Wear Rate} = +4.66816 * \text{Peak current} - 5.27317 * \text{Pulse-on-time} + 5.77492 * \text{Pulse-off-time} + 0.318396 * \text{Peak current} * \text{Pulse-on-time} + 0.297437 * \text{Peak current} * \text{Pulse-off-time} - 0.275958 * \text{Pulse-on-time} * \text{Pulse-off-time} - 0.149943 * \text{Peak current}^2 + 0.404025 * \text{Pulse-on-time}^2 - 1.08127 * \text{Pulse-off-time}^2$$

This equation should not be used to assess the relative impact of each factor, as the coefficients are scaled based on the units of the respective factors and the intercept does not correspond to the center of the design space.

Model Analysis

In response surface methodology (RSM), model analysis involves the evaluation of the fitted model to assess its precision and reliability in predicting the response variable. The primary goal of the model analysis is to examine the performance of the fitted model and identify any influential factors or interactions that affect the response variable.

Optimize Parameter

This involves creating a mathematical model that represents the relationship between the process variables and the desired response. Table 7 lists the constraints of the goal, lower limit, and upper limit of the optimization. The suggested optimized solution, which is provided by the Design Expert software for the output responses in Table 8.

Validation of Results

Validating the results derived from RSM is an essential and crucial stage to guarantee the precision and dependability of the optimization procedure. Validation involves assessing the model's quality and determining its capacity to accurately predict the response variable across various scenarios.

A confirmation test is performed to validate the output responses. This test was carried out based on the suggested parameters provided by Design Expert software. The confirmation test results, which were performed to validate the results, are shown in Table 9.

Table 7. ANOVA for Quadratic model.

	MRR	TWR
R^2	0.9715	0.9568
Adjusted R^2	0.9458	0.9179
Predicted R^2	0.7819	0.6615
p -Value	0.0001	0.0001
Model	Quadratic	Quadratic

Table 8. Constraints in optimization.

No.	Goal	Lower limit	Upper limit	Lower weight	Upper weight	Importance
<i>Input parameters</i>						
A: Peak current	Maximize	5	9	1	1	3
B: Pulse-on-time	Is in range	3	9	1	1	3
C: Pulse-off-time	Is in range	2	4	1	1	3
<i>Output parameters (responses)</i>						
Material removal rate	Maximize	3.899	15.3	1	1	3
Tool wear rate	Minimize	1.324	11.89	1	1	3

Table 9. Suggested optimized solution.

	Peak current	Pulse-on time	Pulse-off time	Material removal rate	Tool wear rate	Desirability	
1	9.000	7.180	3.565	10.017	6.011	0.668	Selected

Table 10. Comparison of predicted results with experimental results.

Parameters		Predicted results at optimum condition	Experimental results	% of deviation
Input	Pulse-on-time (μs)	7	7	
	Pulse-off-time (μs)	4	4	
	Peak current (Ip)	9	9	
Output	Material removal rate ($\text{mm}^3/\text{min.}$)	10.017	10.578	5.30
	Tool wear rate ($\text{mm}^3/\text{min.}$)	6.011	6.567	8.46

Table 11. Confirmation test results.

Input process parameter at optimum condition		
<i>Pulse-on-time</i> (μs): 7	<i>Pulse-off-time</i> (μs): 4	<i>Peak current</i> (Ip): 9
Experimental results–output parameters		
MRR	10.578 $\text{mm}^3/\text{min.}$	
TWR	6.567 $\text{mm}^3/\text{min.}$	

After performing the confirmation test, it needs to be compared with the predicted results, which are given by the software, and the observed percentage of deviation; the required values are under 5% for validation of results, which are listed in Table 10, and confirmation of test results is shown in Table 11.

CONCLUSION

The influence of machining process parameters such as peak current and pulse-on-time on performance criteria such as MRR and TWR while machining AISI 304 by EDM machining technique using brass tool electrodes has been examined. From the set of experimental investigations, the following outcomes were observed during EDM on the AISI 304 material using the brass tool.

1. The peak current (Ip), pulse-on-time (Ton), and pulse-off-time are the most influential factors in the electric discharge machining process, where the peak current has the maximum percentage of contribution to the material removal rate (MRR) as the pulse-off-time MRR decreases.
2. However, when Ip increases above 7A, the TWR increases sharply. A higher current produces a higher discharge energy density, which results in a higher TWR.
3. The highest recorded MRR is 15.1 $\text{mm}^3/\text{min.}$, achieved with a peak current of 9(A), pulse-on-time of 9(μs), and pulse-off-time of 2(μs).
4. The desired MRR was 10.017 $\text{mm}^3/\text{min.}$ and TWR 6.011 $\text{mm}^3/\text{min.}$ was achieved with a peak current of 9(A), a pulse-on-time of 7(μs), and a pulse-off of 4(μs).
5. The TWR gradually decreased with an increase in Toff, which was due to sufficient cooling time around the electrode and less sparking energy.

REFERENCES

1. Thanigaivelan R, Arunachalam R, Natarajan N. Study on influence of electrodes in electric discharge machining. *Recent Pat Mech Eng.* 2015;8(2):161–7. doi:10.2174/2212797608666150610220531.
2. Jahan MP, Wong YS, Rahman M. A comparative experimental investigation of deep-hole micro-EDM drilling capability for cemented carbide (WC-Co) against austenitic stainless steel (SUS 304). *Int J Adv Manuf Technol.* 2010;46:1145–60. doi:10.1007/s00170-009-2167-8.

3. Kaushik N, Jha SK, Anand RS. Effect of input process parameters on MRR in micro EDM drilling of CFRP sheet using RSM. *Mater Today Proc.* 2023. doi:10.1016/j.matpr.2023.10.051.
4. Singh S, Verma M. A parametric optimization of electric discharge drill machine using Taguchi approach. *J Eng Comput Appl Sci.* 2012;1(3):39–48.
5. Ali SM. Influence of electrodes and parameters on micro-EDM drilling performances of 304L stainless steel. 2019 2nd International Conference on Engineering Technology and its Applications (IICETA), Al-Najef, Iraq. 2019. p. 55–60. doi:10.1109/IICETA47481.2019.9012975.
6. Vijayanand MS, Ilangkumaran M. Optimization of micro-EDM parameters using grey-based fuzzy logic coupled with the Taguchi method. *Mater Technol.* 2017;51(6):989–95.
7. Vala K, Shah JB. Optimization of process parameters for AISI 304 using micro-EDM drilling process: a review. *J Mater Metall Eng.* 2023 Dec;13(3):26–37. doi:10.37591/jomme.v13i3.7514.
8. Singh AK, Mahajan R, Tiwari A, Kumar D, Ghadai RK. Effect of dielectric on electrical discharge machining: A review. *IOP Conf Ser Mater Sci Eng.* 2018;377(1):012184. doi:10.1088/1757-899X/377/1/012184.
9. D’Urso G, Giardini C, Ravasio C. Effects of electrode and workpiece materials on the sustainability of micro-EDM drilling process. *Int J Precis Eng Manuf.* 2018;19:1727–34. doi:10.1007/s12541-018-0200-2.
10. Abdudeen A, Abu Qudeiri JE, Kareem A, Ahammed T, Ziout A. Recent advances and perceptive insights into powder-mixed dielectric fluid of EDM. *Micromachines.* 2020;11:754. doi:10.3390/mi11080754. PMID: 32752064.
11. Ramaswamy A, Perumal AV. Multi-objective optimization of drilling EDM process parameters of LM13 Al alloy–10ZrB₂–5TiC hybrid composite using RSM. *J Braz Soc Mech Sci Eng.* 2020;42:1–18.
12. Dewangan S, Deepak Kumar S, Kumar Jha S, Kumar Biswas C. Optimization of micro-EDM drilling parameters of Ti–6Al–4V alloy. *Mater Today Proc.* 2020;33:5481–5. doi:10.1016/j.matpr.2020.03.307.
13. D’Urso G, Maccarini G, Quarto M, Ravasio C. Investigation on power discharge in micro-EDM stainless steel drilling using different electrodes. *J Mech Sci Technol.* 2015;29:4341–9. doi:10.1007/s12206-015-0932-1.
14. Sahoo AK, Mishra DR. Multi-attribute optimization of EDM drilling process parameters on Nitinol using GRA-assisted PSO. In: *Proceedings of the 2nd International Architectural Sciences and Applications Symposium (IArcSAS-2022)*; 2022 Sep 9–11; Baku, Azerbaijan. p. 1259–76.
15. Liu Y, Wang C, Yang X, Sun F, Song J. Fracture behaviour of the 304 stainless steel with micro-EDMed micro-holes. *J Braz Soc Mech Sci Eng.* 2020;42:1–9.